Single Chain Variable Fragments against β-Amyloid (Aβ) Can Inhibit Aβ Aggregation and Prevent Aβ-Induced Neurotoxicity†

Ruitian Liu,‡ Bin Yuan,‡ Sharareh Emadi,‡ Andleeb Zameer,‡ Philip Schulz,‡ Chad McAllister,§ Yuri Lyubchenko,§ Gaddam Goud,|| and Michael R. Sierks*,‡

Department of Chemical and Materials Engineering and Department of Microbiology, Arizona State University, Tempe, Arizona 85287, and Department of Microbiology and Tropical Medicine, The George Washington University, Washington, D.C. 20037

Received January 8, 2004; Revised Manuscript Received March 29, 2004

ABSTRACT: β-Amyloid (Aβ) is a major pathological determinant of Alzheimer's disease (AD). Both active and passive immunization studies have shown that antibodies against Aβ are effective in decreasing cerebral Aβ levels, reducing Aβ accumulation, and attenuating cognitive deficits in animal models of AD. However, the therapeutic potential of these antibodies in human AD patients is limited because of adverse inflammatory reactions and cerebral hemorrhaging associated with the treatments. Here we show that single chain variable fragments (scFv's) represent an attractive alternative to more conventional antibody-based therapeutics to reduce Aβ toxicity. The binding affinities and binding epitopes of two different scFv's to Aβ were characterized using a surface plasmon resonance (SPR) biosensor. An scFv binding the 17−28 region of Aβ effectively inhibited in vitro aggregation of Aβ as determined by thioflavin T (ThT) fluorescence staining and atomic force microscopy (AFM) analysis, while an scFv binding the carboxyl-terminal region of Aβ (residues 29−40) did not inhibit aggregation. The scFv to the 17−28 region when co-incubated with Aβ not only decreased aggregation but also eliminated any toxic effects of aggregated Aβ on the human neuroblastoma cell line, SH-SY5Y. The ability of scFv's to inhibit both aggregation and cytotoxicity of Aβ indicates that scFv's have potential therapeutic value for treating AD.

Alzheimer's disease (AD),[1] a widespread aging-related neurodegenerative disease, is characterized by neuronal loss and the presence of amyloid plaques and neurofibrillary tangles. A primary component of the amyloid plaques is β-amyloid, a short natively unfolded protein (40−42 amino acids), that can assemble into a number of different morphologies including soluble oligomers, protofibrils, and insoluble fibrils, all of which seem to be neurotoxic (*1*−*4*). It is not known what roles the various different morphologies play in the development of AD, although growing evidence suggests the soluble oligomers may be a critical component in AD pathology (*5*−*8*).

Potential therapeutic approaches for AD include reducing Aβ synthesis by targeting the enzymes that process APP to Aβ peptide (*9*−*11*), increasing the clearance of Aβ peptides from brain (*12*, *13*), inhibiting Aβ aggregation (*14*, *15*), decreasing aggregate burden in the brain (*13*, *16*), and reducing inflammation associated with Aβ deposition (*17*, *18*). Active immunization against aggregated Aβ reduced the presence of existing fibrils and inhibited formation of new ones, reducing neurotoxicity (*19*, *20*) and associated memory impairment (*12*, *20*, *21*). Passive immunization with antibodies against Aβ also reduced amyloid deposition (*22*−*24*), cleared existing Aβ plaques, reduced the concentration of soluble peptide (*22*), and reversed Aβ-induced memory deficits (*25*−*27*). Antibodies can alter Aβ aggregation through several different mechanisms including blocking nucleation sites, disrupting preexisting fibrils, or inhibiting fibrillogenesis (*19*). In addition, antibodies can influence Aβ equilibrium between brain and plasma by binding plasma Aβ (*23*, *28*), indirectly drawing Aβ from the brain (*29*, *30*). Finally, since antibodies have been shown to cross from periphery to the brain, they can bind Aβ aggregates in brain tissue and stimulate microglial phagocytosis of the bound Aβ (*13*, *31*−*33*). Because of these different potential methods of clearing Aβ, immunotherapy has great potential for treating or even preventing AD (*34*). Recent clinical trials testing active immunization of human AD patients were canceled due to occurrence of meningoencephalitis in 6% of patients (*34*−*38*). A recent study using intracebroventricular (ICV) injection of anti-Aβ antibody into the third ventricle reduced cerebral plaques, decreased inflammation, and did not trigger microhemorrhage in the brain (*39*), demonstrating the potential benefits of immunotherapy for AD patients providing the inflammatory response can be

† This work was supported in part by grants from the NIH (AG17984), American Health Assistance Foundation, and Alzheimer's Association (IIRG-01-2753).

* Corresponding author. Fax: 480-965-0037. Phone: 480-965-2828. E-mail: sierks@asu.edu.

‡ Department of Chemical and Materials Engineering, Arizona State University.

§ Department of Microbiology, Arizona State University.

|| Department of Microbiology and Tropical Medicine, The George Washington University.

[1] Abbreviations: AD, Alzheimer's disease; Aβ, β-amyloid; scFv, single chain variable fragment; ThT, thioflavin T; SDS−PAGE, sodium dodecyl sulfate−polyacrylamide gel electrophoresis; AFM, atomic force microscopy; SPR, surface plasmon resonance; MTT, 3-(4,5-dimethylthiazol-2-yl)-2,5-diphenyltetrazolium bromide.

10.1021/bi049933o CCC: $27.50
Published on Web 05/12/2004

adequately controlled. Single chain variable domain antibody fragments (scFv's) represent a promising immunotherapeutic approach since they do not contain the antibody Fc region responsible for activating the complement response. In addition to a reduced risk of an inflammatory response, scFv's have a much lower molecular weight than a full antibody, potentially facilitating transfer into the brain.

Antibodies isolated against the amine terminal of Aβ were shown to assist in plaque clearance and reduction of neurotic pathology (*22*, *24*, *40*, *41*) while antibodies against the central region of Aβ do not recognize amyloid plaques but can generally bind soluble Aβ and reduce plaque deposition (*23*). Here we show that scFv's isolated from phage display libraries may be useful alternatives to antibodies as therapeutics for AD. We isolated two scFv's to non-amino-terminal regions of Aβ and show that these scFv's, particularly the one binding the 17−28 region of Aβ, can be used to inhibit both Aβ aggregation and cytotoxicity.

EXPERIMENTAL PROCEDURES

Biopanning Using the ScFv Library. All chemicals were obtained from Sigma-Aldrich (St. Louis, MO) unless otherwise indicated. A naive human single chain variable domain (scFv) phage library (*42*) was obtained from the Medical Research Council (Cambridge, England). Phage selection was performed using four rounds of panning with slight modifications to the procedure originally described by Marks (*43*). Amine-binding 96-well plates (Corning Inc., Corning, NY) were coated with either Aβ1−28 or Aβ1−40 at 10 μg/mL in 50 mM carbonate−bicarbonate buffer, pH 9.6, overnight at 4 °C. The plates were then blocked with 3% milk powder in PBS (10 mM phosphate, 150 mM NaCl, pH 7.4). Aliqouts of the phage library, 10^{12} phage titer units, were incubated with the immobilized peptides for 2 h at room temperature. Bound phage were eluted with 7.18 M triethylamine and neutralized with 1 M Tris-HCl, pH 7.4. Phage titers were determined by infecting *Escherichia coli* cells and using serial dilution on agar plates containing ampicillin (100 μg/mL). Eluted phage were subsequently amplified by infecting *E. coli* TG1 in the presence of helper phage VCSM13 (Stratagene, La Jolla, CA) as described (*43*). The phage were further purified using poly(ethylene glycol)/NaCl precipitation and resuspended in PBS also essentially as described (*43*).

Screening of Positive Clones by Phage ELISA. Individual clones obtained after the fourth round of panning were selected as described (www.mrc.cpe.cam.ac.uk). Amine-binding 96-well plates (Corning) were coated with Aβ1−28 or Aβ1−40 at 10 μg/mL in PBS, pH 9.0, overnight at 4 °C. The plate wells were blocked with 3% milk powder in PBS, pH 7.4. Aliquots of the supernatant obtained from each clone (100 μL/well) were added to individual wells and incubated at room temperature for 2 h. Bound phage were detected using an anti-M13 antibody conjugated to horseradish peroxidase (HRP) (Amersham Pharmacia Biotech, Piscataway, NJ) at 1:5000 dilution. Substrate, 3,3′,5,5′-tetramethylbenzidine (TMB), was added, and the reaction was stopped after 30 min with 2 M H_2SO_4 (VWR, West Chester, PA). Absorbance was calculated as the difference between OD_{650} and OD_{450} values using a Wallac 1420 plate reader (Perkin-Elmer, Gaithersburg, MD).

Production of Soluble ScFv and ELISA. Plasmid DNA from the positive clones identified with phage ELISA was isolated and transformed into the nonsuppressor *E. coli* strain HB2151 (*44*) for production of soluble scFv. Following the procedure as described earlier (*43*), clones were grown, and scFv production was induced by addition of 1 mM isopropyl β-D-thiogalactopyranoside (IPTG). Supernatant samples were obtained by centrifugation at 1500*g*, 30 min at 4 °C. Amine-binding 96-well plates (Corning) were coated with 10 μg/mL of Aβ1−28 or Aβ1−40. Supernatant was added to the wells, and the samples were allowed to stand for 2 h at room temperature. Soluble scFv was detected by an anti-myc antibody conjugated to HRP (Santa Cruz Biotechnology, Santa Cruz, CA) at a 1:500 dilution.

The clone with the highest ELISA readings against Aβ1−28 (H1) and another against Aβ1−40 (C1) were selected for further study. The affinity of the H1 scFv to Aβ1−40 was improved through affinity maturation by randomizing the CDR3 light chain region resulting in H1v2.

Production and Purification of scFv. Soluble scFv's from the two selected clones (H1v2, C1) were produced from 4 L culture volumes grown in four separate 1 L shake flasks as described above. The supernatant and periplasmic fractions from the culture were combined, passed through a 0.2 μm filter (Whatman, Clifton, NJ), and concentrated in a tangential flow filter (Millipore, Bedford, MA) using a 10 kDa cutoff filter (Millipore, Bedford, MA). Concentrated samples were dialyzed overnight against 0.5 M NaCl−PBS and purified either using a HiTrap chelating HP column (Amersham Biosciences, Piscataway, NJ) charged with $NiSO_4$ or using a protein A column as described (*45*). Protein fractions from the $NiSO_4$ column were eluted with 10−25 mM imidazole and dialyzed overnight into PBS. The eluates were analyzed by SDS−PAGE on 15% polyacrylamide gels (Bio-Rad, Hercules, CA).

Aβ Fragments. Aβ1−16, Aβ1−28, and Aβ20−29 were purchased from Bachem (Torrance, CA). Aβ1−40, Aβ17−28, Aβ29−40, and Aβ25−35 were from Biosource (Camarillo, CA). For aggregation experiments, Aβ1−40 was dissolved in 100% 1,1,1,3,3,3-hexafluoro-2-propanal (HFIP) to 2 mg/mL, sonicated in a water bath for 10 min, aliquoted in microcentrifuge tubes, dried under vacuum, and stored at −20 °C. Immediately prior to use, the HFIP-treated Aβ1−40 was dissolved in dimethyl sulfoxide (DMSO) to 20 mg/mL and diluted with PBS to the proper concentration.

Epitope Mapping by Surface Plasmon Resonance (SPR). SPR binding studies were performed using a BIAcore X biosensor (BIAcore, Inc., Uppsala, Sweden). A CM5 sensor chip was activated as recommended by the manufacturer using an equimolar mix of NHS (*N*-hydroxysuccinimide) and EDC [*N*-ethyl-*N*′-(dimethylaminopropyl)carbodiimide], coupled with 20 μg/mL of Aβ40 in pH 4.8 sodium acetate buffer, and then blocked with ethanolamine. Samples of Aβ1−16, Aβ17−28, and Aβ29−40 were each immobilized onto separate CM5 sensor chips (BIAcore). H1v2, C1, and a control scFv against phosphorylase *b* (anti-plb) were diluted to 0.5 mg/mL in the HBS−EP running buffer [0.01 M HEPES, 0.15 M NaCl, 3 mM EDTA, 0.005% (v/v) surfactant P20, pH 7.4] (BIAcore) and injected over the chips containing immobilized Aβ1−16, Aβ17−28, or Aβ29−40 at a flow rate of 10 μL/min. Guanidine hydrochloride (6 M) was used as a regeneration buffer. Data collected represent the value

of the observed response units (RU) obtained in the sample cells minus the RU obtained from a reference cell.

Binding Kinetics. Affinity measurements were performed using a BIAcore X biosensor (BIAcore). ScFv samples were prepared by dilution into HBS−EP buffer (BIAcore). The association and dissociation rate constants (k_a and k_d) were determined using different H1v2 concentrations (624, 832, 1248, 1663, 2494, 3325, and 4988 nM) and C1 concentrations (3977, 5170, 6465, 8167, 12931, and 17241 nM) with HBS−EP as a running buffer at a flow rate of 30 μL/min. Samples of 45 μL were injected. Dissociation data were collected while flowing running buffer for 120 s. Kinetic parameters were evaluated using BIAevaluation 3.1 software (BIAcore).

Thioflavin T (ThT) Fluorescence Assay. An aliquot of the Aβ40 stock solution was diluted to 20 μM in PBS, pH 7.4, and incubated at 37 °C without shaking in a 0.5 mL Eppendorf PCR tube. For initial studies with scFv mixtures, Aβ40 was mixed with equimolar concentrations of each of the two different scFv's to a final Aβ40 concentration of 20 μM. Fluorescence emission of ThT is shifted when it binds to β-sheet aggregate structures such as amyloid fibrils (*46*). Aβ aggregation was measured by periodically removing 30 μL aliquots from the incubation samples and adding them to 2 mL of 5 μM ThT solution (50 mM phosphate buffer, pH 6.5). Fluorescence intensity was monitored at an excitation wavelength of 450 nm and an emission wavelength of 482 nm by a Shimadzu PF-3501PC spectrofluorophotometer using 1 cm light-path quartz cuvettes with both excitation and emission bandwidths of 5 nm. Readings were the results of the average of three values determined by a time scan after subtracting out the fluorescence contribution from free ThT. Each experiment was performed in triplicate. Standard errors were analyzed using Excel software.

Atomic Force Microscope (AFM) Imaging. 1-(3-Aminopropyl)silatrane- (APS-) modified mica was used as an AFM substrate (*47*, *48*). Samples of 5 μL were placed on APS-modified mica for 2 min, rinsed with deionized water, and dried with argon as described earlier (*47*, *48*). Images were acquired in air using a MultiMode SPM NanoScope III system (Veeco/Digital Instruments, Santa Barbara, CA) operating in tapping mode using silicon probes (Olympus). To determine filament widths, either circular plasmid DNA was codeposited onto samples or circular plasmid DNA samples were imaged using a single tip immediately before and after imaging of protofibril samples. DNA is a convenient standard (2 nm wide filaments) to determine the filament diameter of other samples from AFM data. Width measurements were ascertained from the AFM images using Femtoscan software (Advanced Technologies Center, Moscow, Russia). The diameters of fibrils were retrieved from the AFM width data (W) using a simplified expression for W and the filament radii (R_1 and R_2, respectively): $W^2 = 16R_1R_2$. This expression was a simplified version of the expression obtained in assuming a spherical shape of the AFM tip (*49*). Nanoscope software version 5.12 was used to determine the root mean square (rms) values for each of the images.

Cytotoxicity Assay. Human neuroblastoma cells (SH-SY5Y) were maintained in medium with 40% minimal essential medium (MEM), 40% Ham's modification of F-12, 18% fetal bovine serum (FBS), 1% L-glutamine (3.6 mM), and 1% penicillin/streptomycin antibiotics in 5% CO_2 at 37 °C. Cells were harvested from flasks and plated in 96-well polystyrene plates with approximately 1×10^4 cells per 100 μL of medium per well. Plates were incubated at 37 °C for 24 h to allow cells to attach. Aβ40 (20 μM) alone and with equimolar concentrations of H1v2, C1, or control protein BSA were preincubated for 18 days before addition to cell cultures. Aβ samples were diluted with fresh medium to a final Aβ40 concentration of 100 nM in the cell culture well. The same volume of medium was added to control cultures. Plates were then incubated for an additional 72 h at 37 °C. Cell viability was determined using an MTT [3-(4,5-dimethylthiazol-2-yl)-2,5-diphenyltetrazolium bromide] toxicity assay with addition of 10 μL of 5 mg/mL MTT to each well (*51*). After incubation for 3 h at 37 °C, the plates were centrifuged, and the medium was aspirated from each well. MTT dissolvent (100 μL) (0.1 N HCl in 2-propanol) was added to each well. Plates were agitated at room temperature for 15 min to dissolve crystals. The absorbance was measured at 560 nm using a Victor Wallac multiwell assay plate reader (Gaithersburg, MD). Averages from six replicate wells were used for each sample and control, and each experiment was repeated three times. Cell viability was calculated by dividing the absorbance of wells containing samples (corrected for background) by the absorbance of wells containing medium alone (corrected for background).

RESULTS

Phage Selection Using the ScFv Library. Screening of scFv phage libraries was performed using Aβ1−28 or Aβ1−40. Titer units of the eluted phage generally show an increase from approximately 10^4−10^5 after the first round to 10^7 after the fourth round of panning. Phage eluted from the fourth round were used to infect *E. coli* TG1. The strongest binding clone against Aβ40 (C1) as indicated by ELISA was used for further studies. H1v2 was selected on the basis of ELISA as the strongest binding clone generated after one round of affinity maturation of the parent H1.

Epitope Mapping. Both purified scFv's showed a single predominant 29 kDa band by SDS−PAGE (Figure 1A). To determine to which epitope of Aβ each of the scFv binds, we separately fixed Aβ1−16, Aβ17−28, and Aβ29−40 to CM5 chips and then measured the association of the two different scFv samples to each of the peptides. The association curves clearly indicate that H1v2 binds Aβ17−28 (Figure 1C) and C1 binds Aβ29−40 (Figure 1D), while none of the scFv's bound to Aβ1−16 (Figure 1B).

Binding Kinetics of scFv to Monomer Aβ1−40. The association (k_a) and dissociation (k_d) rate constants and the dissociation constants ($K_D = k_a/k_d$) of H1v2 (Figure 2A) and C1 (Figure 2B) for Aβ40 were determined (Table 1). The higher affinity of H1v2 [$K_D = (2.47 \pm 0.122) \times 10^{-7}$ M] compared to C1 [$K_D = (1.63 \pm 0.74) \times 10^{-6}$ M] is primarily due to differences in the association rate constant, k_a, rather than in the dissociation rate constant, k_d.

ScFv Inhibition of Aβ1−40 Aggregation. We investigated the extent to which the scFv's could inhibit aggregation of Aβ using a ThT assay to monitor the Aβ aggregation rate and AFM analysis to follow Aβ aggregate morphology. ThT is a fluorescent dye that specifically binds to fibrillar structures (*46*). Incubation of Aβ1−40 alone shows a time-

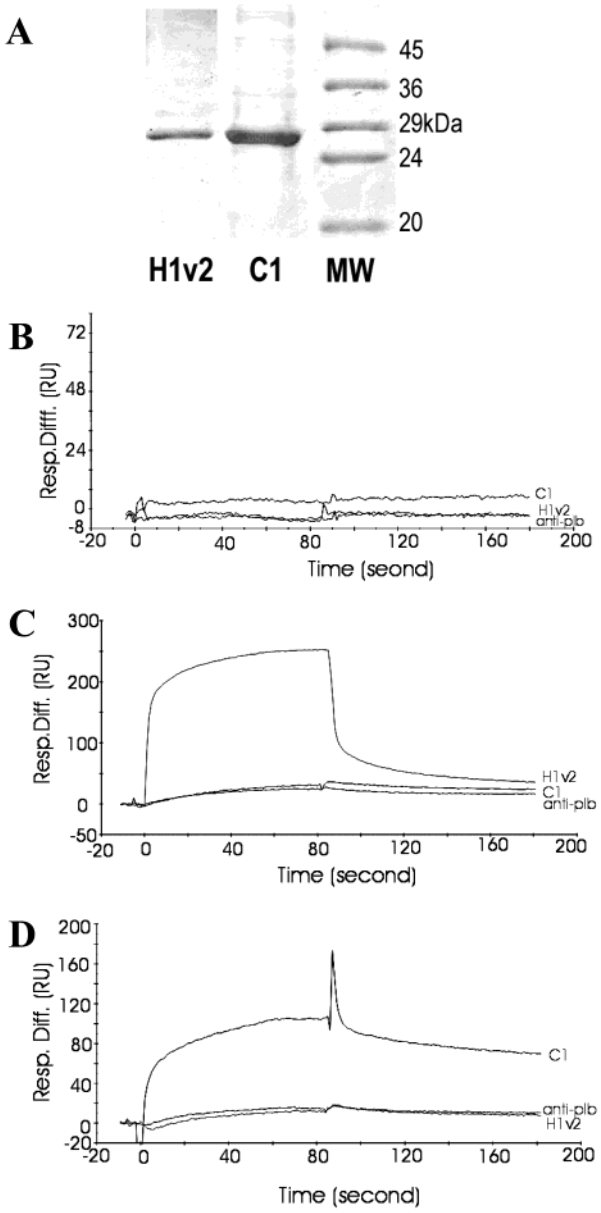

FIGURE 1: SDS−PAGE analysis of purified recombinant scFv antibody and epitope mapping by SPR for scFv. (A) SDS−PAGE analysis of purified recombinant scFv antibody. (B−D) Epitope mapping by SPR. Aβ1−16 (B), Aβ17−28 (C), and Aβ29−40 (D) were coupled to CM5 chips, respectively. H1v2, C1, and anti-plb scFv were passed over the surfaces of ligands at 10 μL/min in HBS−EP running buffer. Data were collected from response units (RU) obtained in the sample cell minus RU from the reference cell.

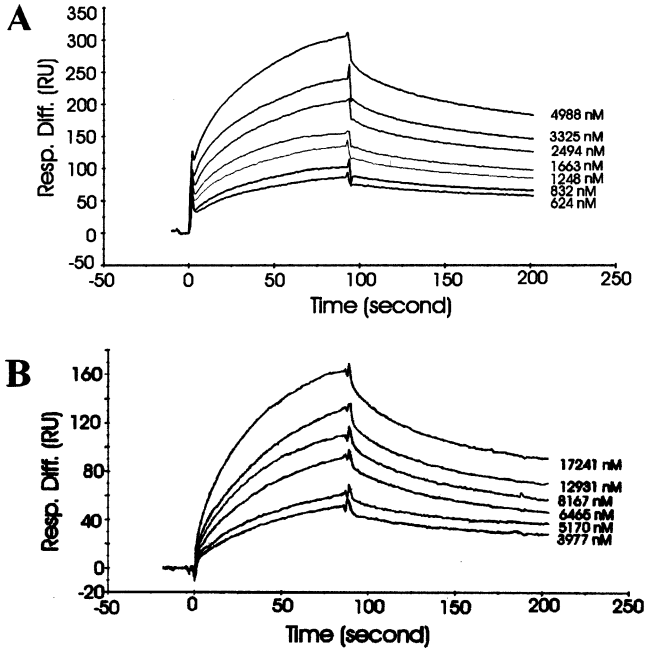

FIGURE 2: Binding kinetics of scFv to Aβ peptide. Binding of scFv to Aβ40 was determined by surface plasmon resonance using a BIAcore X biosensor. Each scFv was passed over a CM5 sensor chip to which Aβ40 had been coupled at a flow rate of 30 μL/min at the following concentrations: H1v2 (4988, 3325, 2494, 1663, 1248, 832, 624 nM) (A); C1 (17241, 12931, 8167, 6465, 5170, 3977 nM) (B). The association and dissociation constants for the scFv were calculated by fitting the data to a single binding model.

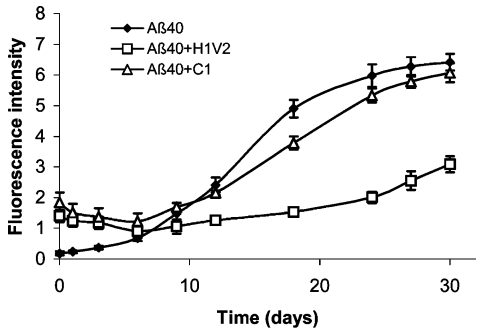

FIGURE 3: Effects of scFv on aggregation of Aβ40. The kinetics of Aβ1−40 (20 μM) fibril formation was monitored by ThT fluorescence in the absence and presence of equimolar concentrations (20 μM) of H1v2 and C1, respectively. The samples were incubated at 37 °C, and 30 μL of the samples was removed periodically and added to 2 mL of 5 μM ThT. Fluorescence intensity was measured at an excitation wavelength of 450 nm and emission wavelength of 482 nm. Readings were the results of the average of three values determined by a time scan after subtracting out the fluorescence contribution from free ThT. Each experiment was performed in triplicate.

dependent increase in fluorescence with a characteristic lag time as the Aβ40 begins to aggregate (Figure 3). Co-incubation of Aβ with equimolar concentrations of each of the two scFv's showed differential effects on aggregation, H1v2 inhibiting aggregation, while C1 had little effect on aggregation (Figure 3). Co-incubation of 20 μM Aβ40 with equimolar concentrations of either a nonspecific control scFv or a nonspecific control protein (phosphorylase *b*) resulted in rapid precipitation of the protein mixtures, precluding determination of aggregation kinetics for these control samples by ThT staining (data not shown) or by AFM.

AFM images were also used to examine morphological differences in the Aβ samples. After incubation for 30 days, the sample containing 20 μM Aβ40 alone formed oligomers and many thin protofibrils (Figure 4A), in agreement with numerous other studies; however, we did not detect the presence of significant amounts of fibrils, likely because of the lower concentrations and higher temperatures used here (*52*−*57*). When Aβ was co-incubated with either of the two

Table 1: Association, Dissociation, and Equilibrium Constants for ScFv Binding to Aβ40

	affinities		
	k_a ($\times 10^3$ M s^{-1})	k_d ($\times 10^{-3}$ s^{-1})	K_D ($\times 10^{-6}$ M)
H1v2	10.1 ± 4.61	2.15 ± 0.138	0.247 ± 0.122
C1	2.15 ± 1.08	3.51 ± 0.63	1.63 ± 0.74

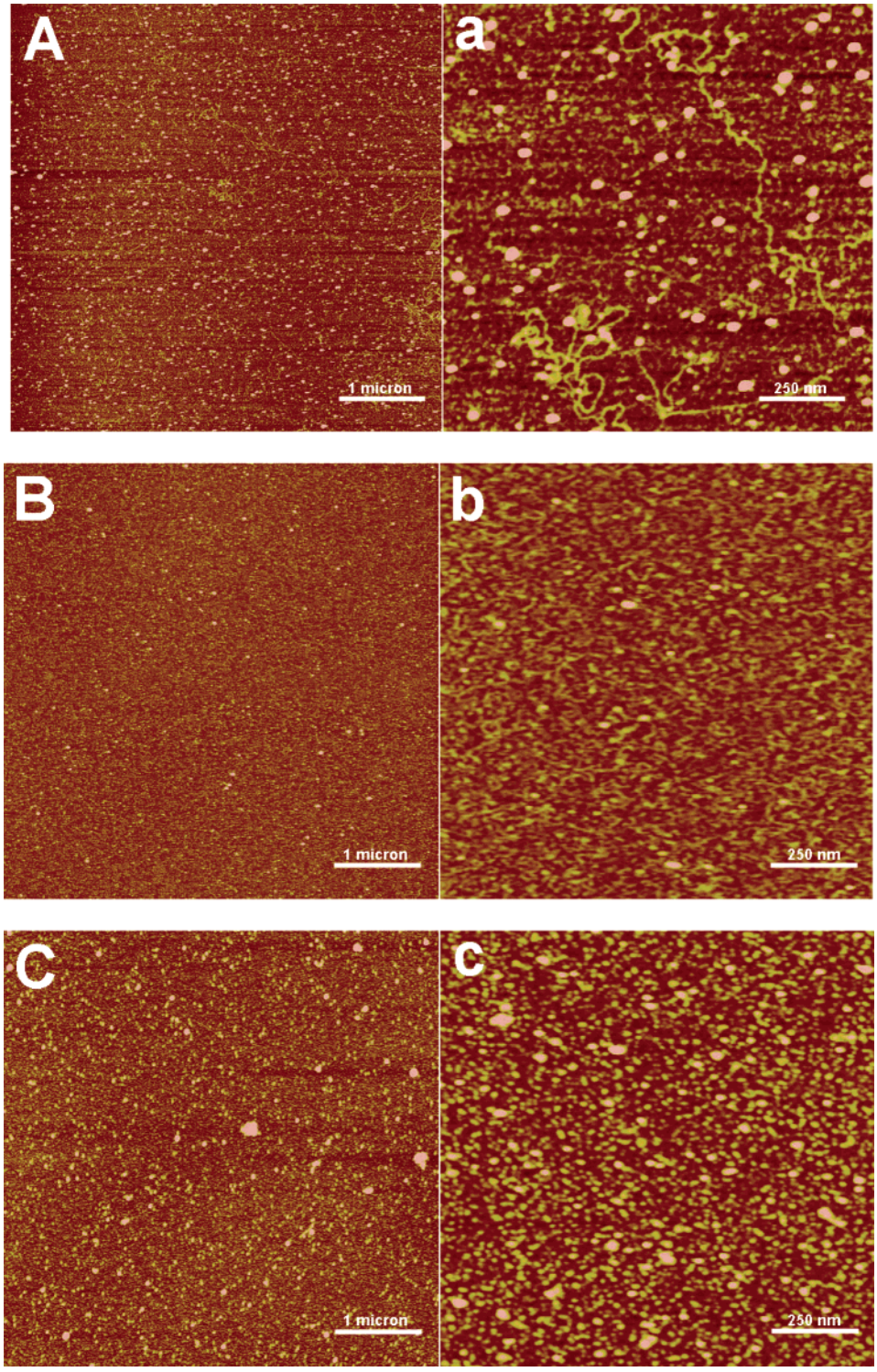

FIGURE 4: AFM images of Aβ1−40 aggregation alone and with added scFv. AFM analysis of Aβ40 incubated alone (A, a), with H1v2 (B, b), or with C1 (C, c) for 30 days at 37 °C. (A−C) Scale bars = 1 μm. (a−c) Scale bars = 250 nm. Z-scale: 100 nm.

scFv's, we could not find evidence of any filaments after 30 days (Figure 4B,C). The aggregates formed in the Aβ40 sample co-incubated with C1 were much larger than those formed in the Aβ40 sample co-incubated with H1v2 (Table 2). Even though the total protein concentration in the Aβ/scFv mixtures was twice as high as that of Aβ40, the total aggregate formation in the Aβ40/scFv mixtures was less than that formed by Aβ40 alone, confirming that binding of H1v2 to Aβ inhibits aggregation of both Aβ40 and H1v2.

Cytotoxicity of Aβ Incubated with or without scFv. Cytotoxicity toward SH-SY5Y cells was measured using samples of Aβ40 alone (20 μM) and equimolar mixtures of Aβ40 with each of the two scFv's after preincubation for 18 days at 37 °C to allow aggregates to form. The samples were diluted to a final Aβ40 concentration of 100 μM and incubated with SH-SY5Y cells for 72 h. The Aβ only aggregated sample showed around a 30% decrease in MTT activity compared to control cells, while the sample co-

Table 2: Height Distribution Analysis (in %) of Aggregates Obtained by AFM Images of Samples of 20 μM Aβ40 Alone and with Equimolar ScFv after Incubation for 30 Days at 37 °C

	molecule height (nm)					
	<0.5	0.5−1.5	1.5−2.5	2.5−0.35	3.5−4.5	4.5−5.5
Aβ40 alone	97.9	0.9	0.4	0.2	0.1	0.1
Aβ40 with H1v2	82.2	14.7	2.0	0.6	0.2	0.1
Aβ40 with C1	58.7	20.0	12.0	6.3	1.4	0.6

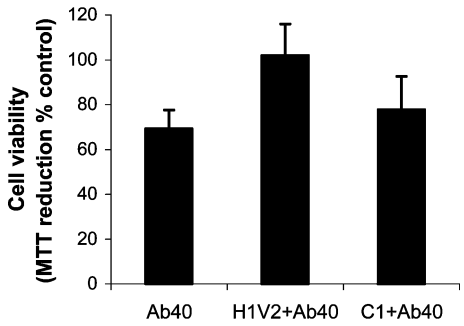

FIGURE 5: Comparison of toxicity of Aβ40 and Aβ40 co-incubated with H1v2 or C1. 20 μM Aβ40 with or without the same concentration of H1v2 or C1 was incubated at 37 °C for 18 days. 10 μL of the samples was added to plates with the final concentration of all samples being 100 nM. The absorbance of dissolved crystals was measured at 560 nm. Data shown are expressed as the percentage of control values from three independent experiments with each experimental value being the average of six trials.

incubated with H1v2 showed no reduction in MTT activity and the sample co-incubated with C1 showed a much smaller increase (~10%) in MTT activity compared to Aβ alone (Figure 5). These results indicate that the H1v2 scFv can provide protection from Aβ-induced toxicity while C1 can provide partial protection.

DISCUSSION

A number of different immunization strategies for clearing Aβ in the brains of AD patients have been proposed or studied (*34*) including active Aβ immunization by either Aβ peptide interval injection (*16*, *20*, *21*, *58*, *59*) or nasal administration with Aβ peptide or phage peptide (*12*, *40*, *60*) and passive immunization with monoclonal or polyclonal antibodies by intravenous or intracerebroventricular peritoneal injection (*13*, *23*−*25*, *37*, *39*, *61*). In general, administration of Aβ antibodies has decreased cerebral amyloid burden and Aβ levels and has also attenuated plaque deposition, neuritic dystrophy, astrogliosis, behavior deficits, and memory loss. However, immunization risks potentially serious side effects as evidenced by the clinical signs and symptoms of meningoencephalitis exhibited by a significant number of AD patients who received active immunization treatments (*34*, *62*). In addition, post-mortem examinations after sustained systemic immunization in animal models of vascular amyloid showed perimicrovascular hemorrhages and inflammation (*36*−*38*), likely due to an autoimmune inflammatory response. Inflammatory reactions and cell lysis may be triggered by T-lymphocyte activation after active immunization (*63*, *64*). In addition, anti-Aβ antibodies may bind epitopes on CNS neurons that can also induce autoimmune reactions (*65*). Finally, microglia activation and phagocytosis of insoluble aggregates may also result in inflammatory responses (*66*). Single chain variable domain antibody fragments (scFv's) do not include the Fc portion of the antibody, and therefore these antibody fragments cannot initiate the complement cascade and limit the inflammatory response upon binding to Aβ peptide. Passive immunization with scFv's also should not stimulate T-lymphocyte activity, which can lyse cells that overproduce Aβ and trigger an inflammatory response (*67*), nor should it activate microglia cells, which could also result in a widespread inflammatory response. Here we demonstrate that scFv's can effectively inhibit Aβ aggregation and also prevent Aβ-induced neurotoxicity. The H1v2 scFv to the central section of Aβ (residues 17−28) inhibited the extent of aggregation of Aβ40 as determined by ThT staining (Figure 3), while H1v2 and C1 (binding the C-terminal region of Aβ) both altered the morphology of the aggregates. Analysis of the images indicate that when Aβ40 is incubated by itself for 30 days, it overwhelmingly formed long thin filaments (Figure 4) having diameters less than 0.5 nm (Table 2). However, when Aβ40 is co-incubated with H1v2, no filaments are observed, and the roughly spherical aggregates formed were predominantly small with over 80% having diameters less than 0.5 nm and an additional 15% with diameters less than 1.5 nm. When Aβ40 is co-incubated with C1, again no filaments are observed; however, the aggregates were substantially larger than observed when Aβ was incubated with H1v2. These results complement and extend a recent report that indicated that a monoclonal antibody directed against the central domain of Aβ (amino acid residues 13−28) appeared to completely prevent the formation of fibrils, while an antibody directed against an N-terminal domain of Aβ (amino acid residues 1−5) merely decreased the rate of fibril formation (*68*).

Epitope mapping studies have traditionally employed immunoblot, ELISA, and immunoprecipitation assays (*69*). Here we show that surface plasmon resonance (SPR) based optical biosensors can be a effective method for epitope mapping, the results clearly showing that the H1v2 scFv specifically binds Aβ17−28 while the C1 scFv specifically binds Aβ29−40. Unlike typical ELISA protocols, SPR does not require a washing step to remove unbound material, and binding is monitored in the presence of unbound substrate, making it possible to characterize low-affinity and transient interactions (*70*).

Previous studies have indicated that regions 17−20 and 30−35 of Aβ play critical roles in the aggregation and cytotoxicity of Aβ (*71*−*77*). The results here provide further evidence for the importance of the 17−20 region, showing that H1v2 strongly inhibits aggregation and toxicity of Aβ. While C1 did not inhibit aggregation, in agreement with previous reports of antibodies to the C-terminal (*13*), binding in this region can still reduce Aβ induced toxicity. The majority of antibodies that reduce plaque burden and that have been isolated from patients in the immunization trials are directed toward the N-terminal residues of the peptide that are exposed and not involved in fibril structure (*13*, *22*). However, a monoclonal antibody raised against Aβ16−24 exhibits high affinity for soluble Aβ and deceases brain Aβ burden in mouse models (*23*), suggesting that the H1v2 scFv isolated here, which binds a similar epitope, may also be effective in clearing Aβ.

There is some controversy as to whether antibody-mediated clearance is dependent on the antibody Fc receptor.

While some studies have indicated Fc-dependent phagocytosis by microglial cells and/or macrophages as being important in clearance (*16*, *22*), other reports indicate that a non-Fc-mediated disruption of plaque structure may also contribute to clearance (*78*, *79*). In the latter studies $F(ab)_2$ fragments prepared from an anti-Aβ antibody reduced amyloid deposits as effectively as the intact antibody when applied topically to the cortex of transgenic mice through a craniotomy. A more recent report indicated that well-characterized FcR-γ chain knock-out mice (FcRγ^{-1}) immunized with Aβ42 exhibited a reduction in Aβ accumulation equivalent to the reduction in deposition seen in Aβ42-immunized, age-matched, FcR-sufficient Tg2576 mice, suggesting that anti-Aβ antibodies can reduce Aβ deposition independent of FcR-mediated phagocytic events (*80*). Further evidence for a mechanism other than FcR-mediated clearance of amyloid is provided by a recent study showing that peripheral administration of two Aβ binding agents, gelsotin and GM-1 ganglioside, had a modest effect on Aβ deposition in transgenic mice (*31*).

Our results indicate that scFv fragments isolated against Aβ can inhibit Aβ aggregation and provide protection against Aβ-induced toxicity. There is strong precedent that the scFv's isolated here may have potential application for treating AD by decreasing amyloid burdens by themselves. In addition, however, these scFv fragments can be combined with a second scFv fragment to generate bispecific scFv's (*81*) that contain an scFv to bind Aβ and inhibit aggregation as shown here and a second scFv to promote clearance of this bound complex from the brain.

ACKNOWLEDGMENT

Cherie Parkhurst is acknowledged for technical assistance.

REFERENCES

1. Klein, W. L., Krafft, G. A., and Finch, C. E. (2001) Targeting small Abeta oligomers: the solution to an Alzheimer's disease conundrum?, *Trends Neurosci. 24*, 219−224.
2. Koo, E. H., Lansbury, P. T., Jr., and Kelly, J. W. (1999) Amyloid diseases: abnormal protein aggregation in neurodegeneration, *Proc. Natl. Acad. Sci. U.S.A. 96*, 9989−9990.
3. Selkoe, D. J. (1999) Translating cell biology into therapeutic advances in Alzheimer's disease, *Nature 399*, A23−A31.
4. Caughey, B., and Lansbury, P. T., Jr. (2003) Protofibrils, Pores, Fibrils, and Neurodegeneration: Separating the Responsible Protein Aggregates from the Innocent Bystanders, *Annu. Rev. Neurosci*.
5. Walsh, D. M., Hartley, D. M., Kusumoto, Y., Fezoui, Y., Condron, M. M., Lomakin, A., Benedek, G. B., Selkoe, D. J., and Teplow, D. B. (1999) Amyloid beta-protein fibrillogenesis. Structure and biological activity of protofibrillar intermediates, *J. Biol. Chem. 274*, 25945−25952.
6. Lashuel, H. A., Hartley, D., Petre, B. M., Walz, T., and Lansbury, P. T., Jr. (2002) Neurodegenerative disease: amyloid pores from pathogenic mutations, *Nature 418*, 291.
7. Nilsberth, C., Westlind-Danielsson, A., Eckman, C. B., Condron, M. M., Axelman, K., Forsell, C., Stenh, C., Luthman, J., Teplow, D. B., Younkin, S. G., Naslund, J., and Lannfelt, L. (2001) The 'Arctic' APP mutation (E693G) causes Alzheimer's disease by enhanced Abeta protofibril formation, *Nat. Neurosci. 4*, 887−893.
8. Kayed, R., Head, E., Thompson, J. L., McIntire, T. M., Milton, S. C., Cotman, C. W., and Glabe, C. G. (2003) Common structure of soluble amyloid oligomers implies common mechanism of pathogenesis, *Science 300*, 486−489.
9. Eriksen, J. L., Sagi, S. A., Smith, T. E., Weggen, S., Das, P., McLendon, D. C., Ozols, V. V., Jessing, K. W., Zavitz, K. H., Koo, E. H., and Golde, T. E. (2003) NSAIDs and enantiomers of flurbiprofen target gamma-secretase and lower Abeta 42 in vivo, *J. Clin. Invest. 112*, 440−449.
10. Esler, W. P., and Wolfe, M. S. (2001) A portrait of Alzheimer secretases—new features and familiar faces, *Science 293*, 1449−1454.
11. Dewachter, I., and Van Leuven, F. (2002) Secretases as targets for the treatment of Alzheimer's disease: the prospects, *Lancet Neurol. 1*, 409−416.
12. Lemere, C. A., Spooner, E. T., LaFrancois, J., Malester, B., Mori, C., Leverone, J. F., Matsuoka, Y., Taylor, J. W., DeMattos, R. B., Holtzman, D. M., Clements, J. D., Selkoe, D. J., and Duff, K. E. (2003) Evidence for peripheral clearance of cerebral Abeta protein following chronic, active Abeta immunization in PSAPP mice, *Neurobiol. Dis. 14*, 10−18.
13. Bard, F., Cannon, C., Barbour, R., Burke, R. L., Games, D., Grajeda, H., Guido, T., Hu, K., Huang, J., Johnson-Wood, K., Khan, K., Kholodenko, D., Lee, M., Lieberburg, I., Motter, R., Nguyen, M., Soriano, F., Vasquez, N., Weiss, K., Welch, B., Seubert, P., Schenk, D., and Yednock, T. (2000) Peripherally administered antibodies against amyloid beta-peptide enter the central nervous system and reduce pathology in a mouse model of Alzheimer disease, *Nat. Med. 6*, 916−919.
14. LeVine, H. (2002) The challenge of inhibiting Abeta polymerization, *Curr. Med. Chem. 9*, 1121−1133.
15. Du, Y., Wei, X., Dodel, R., Sommer, N., Hampel, H., Gao, F., Ma, Z., Zhao, L., Oertel, W. H., and Farlow, M. (2003) Human anti-beta-amyloid antibodies block beta-amyloid fibril formation and prevent beta-amyloid-induced neurotoxicity, *Brain 126*, 1935−1939.
16. Schenk, D., Barbour, R., Dunn, W., Gordon, G., Grajeda, H., Guido, T., Hu, K., Huang, J., Johnson-Wood, K., Khan, K., Kholodenko, D., Lee, M., Liao, Z., Lieberburg, I., Motter, R., Mutter, L., Soriano, F., Shopp, G., Vasquez, N., Vandevert, C., Walker, S., Wogulis, M., Yednock, T., Games, D., and Seubert, P. (1999) Immunization with amyloid-beta attenuates Alzheimer-disease-like pathology in the PDAPP mouse, *Nature 400*, 173−177.
17. Jantzen, P. T., Connor, K. E., DiCarlo, G., Wenk, G. L., Wallace, J. L., Rojiani, A. M., Coppola, D., Morgan, D., and Gordon, M. N. (2002) Microglial activation and beta -amyloid deposit reduction caused by a nitric oxide-releasing nonsteroidal antiinflammatory drug in amyloid precursor protein plus presenilin-1 transgenic mice, *J. Neurosci. 22*, 2246−2254.
18. Jick, H., Zornberg, G. L., Jick, S. S., Seshadri, S., and Drachman, D. A. (2000) Statins and the risk of dementia, *Lancet 356*, 1627−1631.
19. Solomon, B., Koppel, R., Frankel, D., and Hanan-Aharon, E. (1997) Disaggregation of Alzheimer beta-amyloid by site-directed mAb, *Proc. Natl. Acad. Sci. U.S.A. 94*, 4109−4112.
20. Morgan, D., Diamond, D. M., Gottschall, P. E., Ugen, K. E., Dickey, C., Hardy, J., Duff, K., Jantzen, P., DiCarlo, G., Wilcock, D., Connor, K., Hatcher, J., Hope, C., Gordon, M., and Arendash, G. W. (2000) A beta peptide vaccination prevents memory loss in an animal model of Alzheimer's disease, *Nature 408*, 982−985.
21. Janus, C., Pearson, J., McLaurin, J., Mathews, P. M., Jiang, Y., Schmidt, S. D., Chishti, M. A., Horne, P., Heslin, D., French, J., Mount, H. T., Nixon, R. A., Mercken, M., Bergeron, C., Fraser, P. E., St. George-Hyslop, P., and Westaway, D. (2000) A beta peptide immunization reduces behavioural impairment and plaques in a model of Alzheimer's disease, *Nature 408*, 979−982.
22. Bard, F., Barbour, R., Cannon, C., Carretto, R., Fox, M., Games, D., Guido, T., Hoenow, K., Hu, K., Johnson-Wood, K., Khan, K., Kholodenko, D., Lee, C., Lee, M., Motter, R., Nguyen, M., Reed, A., Schenk, D., Tang, P., Vasquez, N., Seubert, P., and Yednock, T. (2003) Epitope and isotype specificities of antibodies to beta-amyloid peptide for protection against Alzheimer's disease-like neuropathology, *Proc. Natl. Acad. Sci. U.S.A. 100*, 2023−2028.
23. DeMattos, R. B., Bales, K. R., Cummins, D. J., Dodart, J. C., Paul, S. M., and Holtzman, D. M. (2001) Peripheral anti-A beta antibody alters CNS and plasma A beta clearance and decreases brain A beta burden in a mouse model of Alzheimer's disease, *Proc. Natl. Acad. Sci. U.S.A. 98*, 8850−8855.
24. Wilcock, D. M., DiCarlo, G., Henderson, D., Jackson, J., Clarke, K., Ugen, K. E., Gordon, M. N., and Morgan, D. (2003) Intracranially administered anti-Abeta antibodies reduce beta-amyloid deposition by mechanisms both independent of and associated with microglial activation, *J. Neurosci. 23*, 3745−3751.

25. Dodart, J. C., Bales, K. R., Gannon, K. S., Greene, S. J., DeMattos, R. B., Mathis, C., DeLong, C. A., Wu, S., Wu, X., Holtzman, D. M., and Paul, S. M. (2002) Immunization reverses memory deficits without reducing brain Abeta burden in Alzheimer's disease model, *Nat. Neurosci. 5*, 452−457.
26. Kotilinek, L. A., Bacskai, B., Westerman, M., Kawarabayashi, T., Younkin, L., Hyman, B. T., Younkin, S., and Ashe, K. H. (2002) Reversible memory loss in a mouse transgenic model of Alzheimer's disease, *J. Neurosci. 22*, 6331−6335.
27. Hock, C., Konietzko, U., Streffer, J. R., Tracy, J., Signorell, A., Muller-Tillmanns, B., Lemke, U., Henke, K., Moritz, E., Garcia, E., Wollmer, M. A., Umbricht, D., de Quervain, D. J., Hofmann, M., Maddalena, A., Papassotiropoulos, A., and Nitsch, R. M. (2003) Antibodies against beta-amyloid slow cognitive decline in Alzheimer's disease, *Neuron 38*, 547−554.
28. DeMattos, R. B., Bales, K. R., Cummins, D. J., Paul, S. M., and Holtzman, D. M. (2002) Brain to plasma amyloid-beta efflux: a measure of brain amyloid burden in a mouse model of Alzheimer's disease, *Science 295*, 2264−2267.
29. Lee, V. M. (2001) Abeta immunization: moving Abeta peptide from brain to blood, *Proc. Natl. Acad. Sci. U.S.A. 98*, 8931−8932.
30. Dodel, R., Hampel, H., Depboylu, C., Lin, S., Gao, F., Schock, S., Jackel, S., Wei, X., Buerger, K., Hoft, C., Hemmer, B., Moller, H. J., Farlow, M., Oertel, W. H., Sommer, N., and Du, Y. (2002) Human antibodies against amyloid beta peptide: a potential treatment for Alzheimer's disease, *Ann. Neurol. 52*, 253−256.
31. Matsuoka, Y., Saito, M., LaFrancois, J., Gaynor, K., Olm, V., Wang, L., Casey, E., Lu, Y., Shiratori, C., Lemere, C., and Duff, K. (2003) Novel therapeutic approach for the treatment of Alzheimer's disease by peripheral administration of agents with an affinity to beta-amyloid, *J. Neurosci. 23*, 29−33.
32. Games, D., Adams, D., Alessandrini, R., Barbour, R., Berthelette, P., Blackwell, C., Carr, T., Clemens, J., Donaldson, T., Gillespie, F., et al. (1995) Alzheimer-type neuropathology in transgenic mice overexpressing V717F beta-amyloid precursor protein, *Nature 373*, 523−527.
33. Brazil, M. I., Chung, H., and Maxfield, F. R. (2000) Effects of incorporation of immunoglobulin G and complement component C1q on uptake and degradation of Alzheimer's disease amyloid fibrils by microglia, *J. Biol. Chem. 275*, 16941−16947.
34. Schenk, D. (2002) Amyloid-beta immunotherapy for Alzheimer's disease: the end of the beginning, *Nat. Rev. Neurosci. 3*, 824−828.
35. Imbimbo, B. P. (2002) Toxicity of beta-amyloid vaccination in patients with Alzheimer's disease, *Ann. Neurol. 51*, 794.
36. Nicoll, J. A., Wilkinson, D., Holmes, C., Steart, P., Markham, H., and Weller, R. O. (2003) Neuropathology of human Alzheimer disease after immunization with amyloid-beta peptide: a case report, *Nat. Med. 9*, 448−452.
37. Pfeifer, M., Boncristiano, S., Bondolfi, L., Stalder, A., Deller, T., Staufenbiel, M., Mathews, P. M., and Jucker, M. (2002) Cerebral hemorrhage after passive anti-Abeta immunotherapy, *Science 298*, 1379.
38. Furlan, R., Brambilla, E., Sanvito, F., Roccatagliata, L., Olivieri, S., Bergami, A., Pluchino, S., Uccelli, A., Comi, G., and Martino, G. (2003) Vaccination with amyloid-beta peptide induces autoimmune encephalomyelitis in C57/BL6 mice, *Brain 126*, 285−291.
39. Chauhan, N. B., and Siegel, G. J. (2003) Intracerebroventricular passive immunization with anti-Abeta antibody in Tg2576, *J. Neurosci. Res. 74*, 142−147.
40. Frenkel, D., Katz, O., and Solomon, B. (2000) Immunization against Alzheimer's beta-amyloid plaques via EFRH phage administration, *Proc. Natl. Acad. Sci. U.S.A. 97*, 11455−11459.
41. Town, T., Tan, J., Sansone, N., Obregon, D., Klein, T., and Mullan, M. (2001) Characterization of murine immunoglobulin G antibodies against human amyloid-beta1−42, *Neurosci. Lett. 307*, 101−104.
42. Nissim, A., Hoogenboom, H. R., Tomlinson, I. M., Flynn, G., Midgley, C., Lane, D., and Winter, G. (1994) Antibody fragments from a 'single pot' phage display library as immunochemical reagents, *EMBO J. 13*, 692−698.
43. Marks, J. D., Hoogenboom, H. R., Bonnert, T. P., McCafferty, J., Griffiths, A. D., and Winter, G. (1991) By-passing immunization. Human antibodies from V-gene libraries displayed on phage, *J. Mol. Biol. 222*, 581−597.
44. Carter, P., Bedouelle, H., and Winter, G. (1985) Improved oligonucleotide site-directed mutagenesis using M13 vectors, *Nucleic Acids Res. 13*, 4431−4443.
45. Wu, H., Goud, G. N., and Sierks, M. R. (1998) Artificial antibodies for affinity chromatography of homologous proteins: application to blood clotting proteins, *Biotechnol. Prog. 14*, 496−499.
46. LeVine, H., III (1993) Thioflavine T interaction with synthetic Alzheimer's disease beta-amyloid peptides: detection of amyloid aggregation in solution, *Protein Sci. 2*, 404−410.
47. Shlyakhtenko, L. S., Miloseska, L., Potaman, V. N., Sinden, R. R., and Lyubchenko, Y. L. (2003) Intersegmental interactions in supercoiled DNA: atomic force microscope study, *Ultramicroscopy 97*, 263−270.
48. Shlyakhtenko, L. S., Potaman, V. N., Sinden, R. R., Gall, A. A., and Lyubchenko, Y. L. (2000) Structure and dynamics of three-way DNA junctions: atomic force microscopy studies, *Nucleic Acids Res. 28*, 3472−3477.
49. Bustamante, C., Vesenka, J., Tang, C. L., Rees, W., Guthold, M., and Keller, R. (1992) Circular DNA molecules imaged in air by scanning force microscopy, *Biochemistry 31*, 22−26.
50. Lee, H. C., Yin, P. H., Lu, C. Y., Chi, C. W., and Wei, Y. H. (2000) Increase of mitochondria and mitochondrial DNA in response to oxidative stress in human cells, *Biochem. J. 348* (Part 2), 425−432.
51. Shearman, M. S., Hawtin, S. R., and Tailor, V. J. (1995) The intracellular component of cellular 3-(4,5-dimethylthiazol-2-yl)-2,5-diphenyltetrazolium bromide (MTT) reduction is specifically inhibited by beta-amyloid peptides, *J. Neurochem. 65*, 218−227.
52. Stine, W. B., Jr., Dahlgren, K. N., Krafft, G. A., and LaDu, M. J. (2003) In vitro characterization of conditions for amyloid-beta peptide oligomerization and fibrillogenesis, *J. Biol. Chem.278*, 11612−11622.
53. Shimizu, T., Fukuda, H., Murayama, S., Izumiyama, N., and Shirasawa, T. (2002) Isoaspartate formation at position 23 of amyloid beta peptide enhanced fibril formation and deposited onto senile plaques and vascular amyloids in Alzheimer's disease, *J. Neurosci. Res. 70*, 451−461.
54. Gorman, P. M., Yip, C. M., Fraser, P. E., and Chakrabartty, A. (2003) Alternate aggregation pathways of the Alzheimer beta-amyloid peptide: Abeta association kinetics at endosomal pH, *J. Mol. Biol. 325*, 743−757.
55. Harper, J. D., Wong, S. S., Lieber, C. M., and Lansbury, P. T. (1997) Observation of metastable Abeta amyloid protofibrils by atomic force microscopy, *Chem. Biol. 4*, 119−125.
56. Harper, J. D., Wong, S. S., Lieber, C. M., and Lansbury, P. T., Jr. (1999) Assembly of A beta amyloid protofibrils: an in vitro model for a possible early event in Alzheimer's disease, *Biochemistry 38*, 8972−8980.
57. Nichols, M. R., Moss, M. A., Reed, D. K., Lin, W. L., Mukhopadhyay, R., Hoh, J. H., and Rosenberry, T. L. (2002) Growth of beta-amyloid(1−40) protofibrils by monomer elongation and lateral association. Characterization of distinct products by light scattering and atomic force microscopy, *Biochemistry 41*, 6115−6127.
58. Lambert, M. P., Viola, K. L., Chromy, B. A., Chang, L., Morgan, T. E., Yu, J., Venton, D. L., Krafft, G. A., Finch, C. E., and Klein, W. L. (2001) Vaccination with soluble Abeta oligomers generates toxicity-neutralizing antibodies, *J. Neurochem. 79*, 595−605.
59. Spooner, E. T., Desai, R. V., Mori, C., Leverone, J. F., and Lemere, C. A. (2002) The generation and characterization of potentially therapeutic Abeta antibodies in mice: differences according to strain and immunization protocol, *Vaccine 21*, 290−297.
60. Weiner, H. L., Lemere, C. A., Maron, R., Spooner, E. T., Grenfell, T. J., Mori, C., Issazadeh, S., Hancock, W. W., and Selkoe, D. J. (2000) Nasal administration of amyloid-beta peptide decreases cerebral amyloid burden in a mouse model of Alzheimer's disease, *Ann. Neurol. 48*, 567−579.
61. Mohajeri, M. H., Saini, K., Schultz, J. G., Wollmer, M. A., Hock, C., and Nitsch, R. M. (2002) Passive immunization against beta-amyloid peptide protects central nervous system (CNS) neurons from increased vulnerability associated with an Alzheimer's disease-causing mutation, *J. Biol. Chem. 277*, 33012−33017.
62. Senior, K. (2002) Dosing in phase II trial of Alzheimer's vaccine suspended, *Lancet Neurol. 1*, 3.
63. Grubeck-Loebenstein, B., Blasko, I., Marx, F. K., and Trieb, I. (2000) Immunization with beta-amyloid: could T-cell activation have a harmful effect?, *Trends Neurosci. 23*, 114.
64. Monsonego, A., Imitola, J., Zota, V., Oida, T., and Weiner, H. L. (2003) Microglia-mediated nitric oxide cytotoxicity of T cells

following amyloid beta-peptide presentation to Th1 cells, *J. Immunol. 171*, 2216−2224.
65. Rohn, T. T., Ivins, K. J., Bahr, B. A., Cotman, C. W., and Cribbs, D. H. (2000) A monoclonal antibody to amyloid precursor protein induces neuronal apoptosis, *J. Neurochem. 74*, 2331−2342.
66. Rogers, J., and Shen, Y. (2000) A perspective on inflammation in Alzheimer's disease, *Ann. N.Y. Acad. Sci. 924*, 132−135.
67. Marx, F., Blasko, I., Zisterer, K., and Grubeck-Loebenstein, B. (1999) Transfected human B cells: a new model to study the functional and immunostimulatory consequences of APP production, *Exp. Gerontol. 34*, 783−795.
68. Legleiter, J., Czilli, D. L., Gitter, B., DeMattos, R. B., Holtzman, D. M., and Kowalewski, T. (2004) Effect of Different Anti-Abeta Antibodies on Abeta Fibrillogenesis as Assessed by Atomic Force Microscopy, *J. Mol. Biol. 335*, 997−1006.
69. Takeuchi, K., Turley, S. J., Tan, E. M., and Pollard, K. M. (1995) Analysis of the autoantibody response to fibrillarin in human disease and murine models of autoimmunity, *J. Immunol. 154*, 961−971.
70. Rich, R. L., and Myszka, D. G. (2003) Spying on HIV with SPR, *Trends Microbiol. 11*, 124−133.
71. Urani, A., Romieu, P., Roman, F. J., and Maurice, T. (2002) Enhanced antidepressant effect of sigma(1) (sigma(1)) receptor agonists in beta(25−35)-amyloid peptide-treated mice, *Behav. Brain Res. 134*, 239−247.
72. Pike, C. J., Walencewicz-Wasserman, A. J., Kosmoski, J., Cribbs, D. H., Glabe, C. G., and Cotman, C. W. (1995) Structure−activity analyses of beta-amyloid peptides: contributions of the beta 25−35 region to aggregation and neurotoxicity, *J. Neurochem. 64*, 253−265.
73. Balbach, J. J., Ishii, Y., Antzutkin, O. N., Leapman, R. D., Rizzo, N. W., Dyda, F., Reed, J., and Tycko, R. (2000) Amyloid fibril formation by A beta 16−22, a seven-residue fragment of the Alzheimer's beta-amyloid peptide, and structural characterization by solid-state NMR, *Biochemistry 39*, 13748−13759.
74. Ma, B., and Nussinov, R. (2002) Stabilities and conformations of Alzheimer's beta-amyloid peptide oligomers (Abeta 16−22, Abeta 16−35, and Abeta 10−35): Sequence effects, *Proc. Natl. Acad. Sci. U.S.A. 99*, 14126−14131.
75. Soto, C. (2003) Unfolding the role of protein misfolding in neurodegenerative diseases, *Nat. Rev. Neurosci. 4*, 49−60.
76. Hiruma, H., Katakura, T., Takahashi, S., Ichikawa, T., and Kawakami, T. (2003) Glutamate and Amyloid {beta}-Protein Rapidly Inhibit Fast Axonal Transport in Cultured Rat Hippocampal Neurons by Different Mechanisms, *J. Neurosci. 23*, 8967−8977.
77. George, J. M., Jin, H., Woods, W. S., and Clayton, D. F. (1995) Characterization of a novel protein regulated during the critical period for song learning in the zebra finch, *Neuron 15*, 361−372.
78. Solomon, B. (2001) Immunotherapeutic strategies for prevention and treatment of Alzheimer's disease, *DNA Cell Biol. 20*, 697−703.
79. Bacskai, B. J., Kajdasz, S. T., McLellan, M. E., Games, D., Seubert, P., Schenk, D., and Hyman, B. T. (2002) Non-Fc-mediated mechanisms are involved in clearance of amyloid-beta in vivo by immunotherapy, *J. Neurosci. 22*, 7873−7878.
80. Das, P., Howard, V., Loosbrock, N., Dickson, D., Murphy, M. P., and Golde, T. E. (2003) Amyloid-beta immunization effectively reduces amyloid deposition in FcRgamma-/- knock-out mice, *J. Neurosci. 23*, 8532−8538.
81. Hudson, P. J., and Kortt, A. A. (1999) High avidity scFv multimers; diabodies and triabodies, *J. Immunol. Methods 231*, 177−189.

BI049933O